Journal of Metals, Materials and Minerals, Vol. 31, No. 4, pp. 151-157, 2021

Luminescent properties of polyaniline capped Mn doped ZnS quantum dots

Anju BALA[1,*], Rajeev SEHRAWAT[1], Anil Kumar SHARMA[1], and Pardeep SONI[2]

[1] *Department of Physics, Maharishi Markandeshwar (Deemed to be University) (MMDU), Mullana, Ambala 133207, Haryana, India*
[2] *Center of nanotechnology, Indian Institute of Technology Roorkee, Roorkee 247667, Uttrakhand, India*

***Corresponding author e-mail:** anjukamboj134@gmail.com

Received date:
27 August 2021
Revised date
17 October 2021
Accepted date:
27 October 2021

Keywords:
Polyaniline;
Zinc sulfide nanoparticles;
Luminescent properties;
Ab-initio computation

Abstract

Synthesis of polyaniline capped and Mn doped quantum dots are performed with co-precipitation tech. while structural, optical and morphological properties have been carried out by using Fourier Transform Infrared Spectroscopy (FTIR), X-Ray Diffraction (XRD) study, photoluminescent (PL), absorption spectroscopy and High-Resolution Transmission Electron Microscopy (HR-TEM). Particles size is nearly 2 nm calculated using XRD analysis and nearly 2.5 nm as estimated from HR-TEM study. FTIR spectra confirm that ZnS and polyaniline interact through S-H vibrations. The absorption spectra analysis reflects the occurrence of blue shift at the peak of absorption along with the enhanced band gap of polyaniline capped ZnS(Mn) nanocomposites as compare to bulk ZnS, this confirms *quantum confinement effect.*

Computation using DFT (B3LYP) 6-31G method shows a strong electronic interaction between the Zn and N creating a large dipole moment of 13.3586 Debye on the interacting site. The red shift has been shown in PL spectra with increasing conc. of polyaniline in ZnS(Mn) *quantum dots*. The optical behavior of polymer capped ZnS(Mn) *quantum dots* has been maintained by these PL and other properties due to which flexibility of the nanostructure material may get improved and make it highly preferable for application in foldable display devices and laser diode.

1. Introduction

The physics of nanosized materials has been remained much interesting area in the past few decades because of their peculiar size-dependent structural, mechanical, electronic, photoconductor and optical-mechanical properties [1-4]. The morphologies of nanomaterial such as nanotubes, nano-wires, nano-rods etc. have a significant impact on its different physical properties [5]. The different particle morphologies can be developed using various synthesis techniques which include sol-gel, chemical bath deposition, electrochemical vapor deposition, co-precipitation and hydrothermal method [6-10]. The chemical co-precipitation method, which is mostly used due to its low synthesis cost along with better product and eco-friendly nature [11], forms spherical morphologies to the nanoparticles as it is a bottom-up technique in which molecule to molecule addition takes place.

Zinc sulfide (ZnS), a compound semiconductor has a large optical band gap (3.67ev) due to which it remains a promising material for different applications in electroluminescence, light-emitting diode, solar cells, photo luminescent, optoelectronic devices, sensors, lasers and bio-devices [12-14]. As a result of its promising optical properties, low cost, environmentally friendly and simple production, ZnS has gained popularity as a luminescent material. In addition, it is suitable for various doping agents as a host material [15]. The structural, electrical and optical properties of ZnS can be greatly improved with doping agent, particle size reduction and surface coating on the core quantum dots (QDs) [16,17]. The doped ZnS nanoparticles using different elements such as Cu, Pb, Co, Ni, Mn, etc. have been received a lot of attention in recent research [18-22]. From all of the above, Mn ions doping is more notable than others because of its similar physical and chemical properties to ZnS along with broad emission peaks having characteristics emission from $4T_1$–$6A_1$ transition in yellow-orange range [23]. Particle size reduction of the ZnS below the exciton Bohr radius results strong *quantum confinement effects* which leads to interesting optical properties. But in doing so, in the QDs, red shift occurs in the peak of absorption band and long recombination time of order of micron second compared to that of nanosecond. These limitations arise due to recombination of local surface carrier due to which trap centers are created on the surface of QDs having energy less than that of band gap [24]. The local surface defects are very prominent for the QDs as higher fraction of atoms lies on the surface at small dimensions. In order to remove these trap centers, surface coating is essential to passivate the surface of QDs [25]. Also, optical properties of ZnS(Mn) QDs can be tuned by a surface coating of hetero structure type of core-shell QDs. The efficiency of these materials can be improved by using material have higher band gap compared to that of core QDs [26]. Recent researches have been carried out on the combination of inorganic doped semiconductor metal oxide and organic conductive polymer to form nanocomposites with improves photo luminescent efficiency as opposed to their counterparts. These nanocomposites have proved their superiority in numerous applications including LEDs, chromatography, secondary batteries, electro chrome devices and gas sensors etc. [27-30].

Polyaniline(PANI) is a organic polymer that has been used in research for variety of reasons including simple synthesis, higher

conductivity and low raw materials cost [31]. Moreover, the optical band gap of pristine polyaniline is 3.94 eV which is higher than ZnS core QDs [32]. In literature, very few studies show that the doping of transition metal ions and capping of organic polymers can tune the optical properties of ZnS [33]. However, the effect of doping and capping is still under consideration and remains controversial.

We present a brief investigation about the luminescent and structural properties of PANI capped and Mn doped (PANI/ZnS(Mn)) nanocomposites with different conc. of PANI by using the oxidation polymerization method of aniline monomers. The main benefit of polymer capping is the increase in flexibility of ZnS(Mn) due to which these composite material may be used in the application of foldable display devices.

2. Experimental

2.1 Chemicals and reagents

Zinc acetate ($ZnC_4H_6O_4$) AR (99.5%) and ammonium peroxydisulfate (APS) ($(NH_4)_2S_2O_8$) GR (98%) were purchased from sd-fine chem. Aniline ($C_6H_5NH_2$) AR (99.5%), $FeCl_3$ (GR 98%), N-methyl-2pyrrolidone (C_5H_9NO) GR (99%) are bought from CDH and purified as required in the investigation. Sodium sulfide (Na_2S) GR (98%), Hydrochloric acid (HCL) GR 6+ (30%) and Manganese acetate tetrahydrate ($C_6H_6M_gO_4.4H_2O$) GR (98%) were bought from Loba Chemie. Ethanol (C_2H_5OH) GR (99.8%) was bought from Merek,, INDIA.

2.2 Synthesis of manganese doped ZnS

The co-precipitation method was used to synthesize ZnS(Mn) QDs. Sodium sulfide, zinc acetate and manganese acetate were taken as source material for S, Zn and Mn accordingly. The sol. of manganese acetate and distilled water, in which manganese acetate (0.6373 g) is mixed in 20 mL deionized (DI) water, is drop wise added to solution of zinc acetate (11.19 g) and DI water (20 mL followed by stirring for 20 min. Another sol. of sodium sulfide (3.98 g) and DI water (50 mL) is mixed drop wise to the above sol. for the growth of Mn-doped ZnS. This results in the instant formation of white precipitate after which the sol. was stirred continuously for 20 min. to complete the chemical reaction. The precipitates were centrifuged and washed several times with DI water. Obtained material oven for 12 h at the temperature of 60°C and then particles of material were de-agglomerated by pestle and mortar to produce a powder of a very fine quality.

2.3 Synthesis of polyaniline

For the synthesis of polyaniline, 5 mL of aniline monomer were drop wise added in 100 mL 2M HCL. Thereafter, this sol. was ice-cooled to ~3°C. After 30 minutes, 8 g of APS dissolved in 40 mL DI water is added drop by drop to the above sol. followed with continuous stirring. Formation of green color precipitate takes place with the addition of APS solution. Stirring was continued for 24 h to complete the polymerization process. After that, the sol. was washed and filtered many times with DI water. Obtained green color residue was dried for 12 h in the vacuum oven at 60°C. Dried samples were grinded to get polyaniline in powder form.

2.4 Synthesis of polyaniline capped Mn-doped ZnS nanocomposites (PANI/ZnS(Mn))

PANI capped ZnS(Mn) nanocomposites were synthesized by deposition of different amounts of polyaniline using the in-situ polymerization method. Initially, 3.66 g of ZnS(Mn) QDs were wetted with 0.0183 mL, 0.1647 mL, 0.3294 mL and 0.4941 mL of aniline monomer for 15 min. so that polymerization could start on the surface of QDs. 100 mL deionized water was added to above sol. followed by stirring for 30 min. 1.6 wt% (aniline) APS was dissolved in DI water (40 mL) and then added drop wise to the above sol. along with continuous stirring. This was continued for 24 h for the proper growth of polymer chains. The obtained sol. was filtered and washed sometimes using DI water. Obtained black residue was dried for overnight in a vacuum oven. The dried material was de-agglomerated with mortal-pestle to obtained powder form of polyaniline capped ZnS(Mn) nanoparticles.

2.5 Characterizations

XRD analysis was carried out on Panalytical's Pro (x-ray diffractrometer) by using Cuk_α radiation with wavelength of 1.54 Å and a scan rate of 1.5° per min., for identification of crystal structure. Morphology of the samples was examined by using (TECNAI G20 HR-TEM) with an operating voltage of 200KV. The PL and absorption spectra were recorded on a multi mode micro plate reader hybrid (Synergy H_1). The FTIR spectra of the samples were studied by using (IRAFFNITY-21CE). Electrostatic potential surface analysis of the synthesized samples was analyzed using ab-initio calculation with G-03 and Gauss view 4.1 computed using DFT (B3LYP) 6-31G technique.

3. Results and discussion

3.1 XRD analysis

XRD pattern of ZnS(Mn) and PANI/ZnS(Mn) QDs with different conc. of PANI(1%, 3%, 6%) is shown in Figure 1.

The spectra show three different peaks at 2θ = 28.7°, 48.5° and 56.5° analogue to the planes (111), (220), and (311) of cubic structure (matched to JCPDS No.01-080-0020) of ZnS structure respectively.

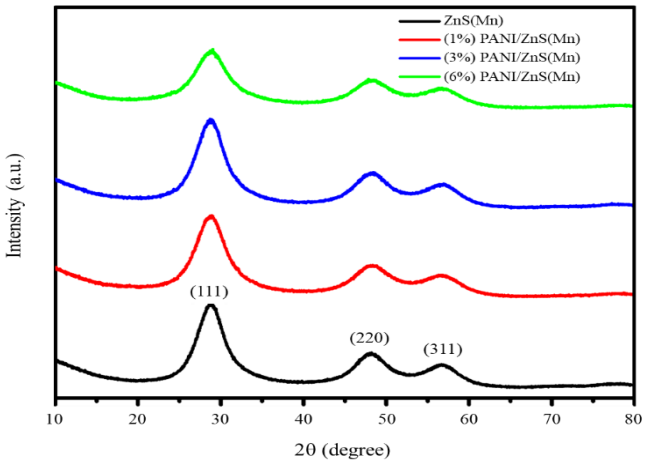

Figure 1. XRD pattern of ZnS(Mn) and PANI/ZnS(Mn) samples.

XRD spectra of PANI/ZnS(Mn) nanocomposite does not show any other extra peak which reveals the absence of any other impurity phase. It was also observed from the diffraction pattern that with the increase of PANI amount, the peak intensities corresponding to the ZnS structure get decreased. This may be due to the hindrance provided by the PANI chains capped on the ZnS(Mn) nanoparticles. Mean crystalline sizes are estimated with Scherrer's Equation (1):

$$d = k\lambda / \beta cos\theta \qquad (1)$$

Where k is constant having a numerical value of 0.94, λ (wavelength) wavelength used in the X-ray diffraction, β is full width half maximum at highest peak of the spectra, d is crystallite size and 2θ is Bragg's angle [34]. The estimated particle size of uncapped sample is ~2.0 nm calculated by considering highest peak of diffraction pattern, which is nearly same as that of the PANI/ZnS(Mn) nanoparticles after PANI coating. This shows that dilution do not occur in the particles throughout the growth process of polyaniline. Since the particle size is less than that of ZnS Bohr's radius of the exciton (which is equal to 2.5 nm), a strong *quantum confinement effect* is considered for these samples.

3.2 FTIR studies

Figure 2 shows the FTIR spectra of Polyaniline (a) and polyaniline capped ZnS(Mn) nanocomposites (b). FTIR spectra of polyaniline demonstrate the different bands at 626.87, 732.95, 1147.65, 1363.67, 1456.26, 1570.06, 2872.01, and 2945.30 cm^{-1} which reveals the formation of pure polyaniline. The characteristics vibrational bands at 1570.06 $cm^{-1}$and 1456.26 cm^{-1} arise due to C=C stretching vibrations of quinonoid ring (QR) and benzenoid ring (BR) of aromatic in PANI [35]. In addition, a very weak peak observes at 1147.55 cm^{-1} due to formation of polarons or by polarons which originates due to hydrogen ions on PANI [36]. Apart from this, a sharp band present at 1363.67 cm^{-1} may be caused by the C-N stretching vibrations of aromatic amines. Occurrence of another peak at 626.87 cm^{-1} assigned to the C-C bonding of aromatic benzene rings [37]. The O-H stretching vibration of PANI is identified by a very sharp and strong peak which is observed at 2945.3 cm^{-1}.

FTIR spectra peaks of the above functional groups for PANI/ ZnS(Mn) nanocomposites are slightly shifted as compared to pure PANI. The shift of vibration frequency may be due to the disturbance observed because of interaction of PANI with the ZnS(Mn) QDs.

There is shift of peaks from 626.8, 1147.65, 1363.67, 1456.26, and 2945.30 cm^{-1} to 619.15, 1159.22, 1371.3, 1458.18, and 2933.73 cm^{-1} respectively in PANI capped ZnS(Mn) nanocomposites. Moreover, the FTIR spectra of PANI/ZnS(Mn) nano-composites show three new broad peaks at 1789.94, 2341.56, and 3597.24 cm^{-1}. Very significant broad peak at 3597.24 cm^{-1} is assigned to the O-H vibration of moisture in the samples. There is a shift from 1456.26 cm^{-1} to 1458.18 cm^{-1} and this shift indicates that deformation is caused by interactions between ZnS and PANI. The appearance of another very sharp as well as broad band at 2341.56 cm^{-1} is may be due to S-H vibration [38]. These results of the FTIR spectra indicate that ZnS(Mn) *quantum dots* interact with PANI.

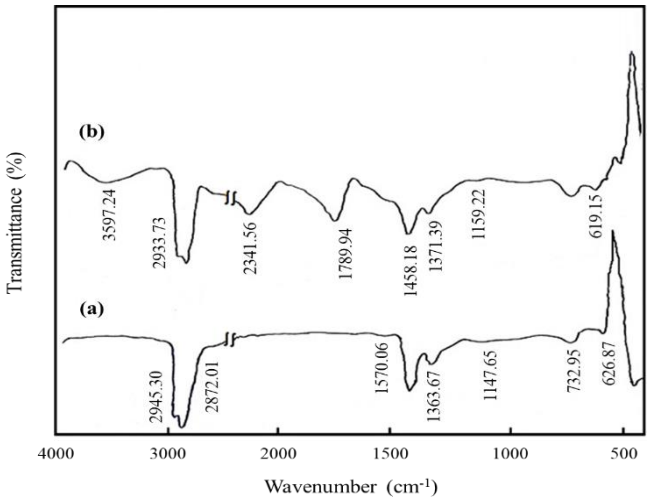

Figure 2. FTIR pattern of PANI and PANI capped ZnS(Mn) QDs.

3.3 UV-visible spectroscopy

The absorption spectra of ZnS(Mn) and PANI/ZnS(Mn) PANI nanoparticles having a wavelength in between the range of 250 nm to 750 nm are shown in Figure 3(a). From the figure, a strong absorption is absorbed at the wavelength of 295 nm, 310 nm, 335 nm, 320 nm and 400 nm for uncapped ZnS(Mn), PANI capped ZnS(Mn) (1 wt%, 3 wt%, 6 wt% and 9 wt% of PANI) nanocomposites respectively.

Energy band gaps of all the samples are found by absorbance data with use of Tauc's Equation (2):

$$(\alpha h\upsilon)^2 = A\left(h\upsilon - E_g\right) \qquad (2)$$

Where α is the coefficient of absorption, h is the Plank's constant, υ is frequency of photons, A is proportionality constant and E_g is optical band gap energy. The value of band gap for direct transition can be fixed by extrapolating the straight line portion of $(\alpha h\upsilon)^2$ versus $h\upsilon$ graphs for uncapped ZnS(Mn)and PANI capped ZnS(Mn) QDs [39] shown in Figure 3(b). As the calculated bandgaps for all the PANI/ ZnS(Mn) nanocomposites is higher than that of ZnS (which is 3.67 eV) [40] listed as in Table 1, therefore these samples exhibit *quantum confinement effect* along with the blue shift. This result of absorption spectra is well matched with the earlier reported studies in respect of different capping agents with ZnS(Mn) nanoparticles (41,42).

However, if capping is beyond the limit of 6 wt%, the observed band gap reduces to 2.6 eV which is below 3.67 eV, this occurs because addition of higher fraction of polyaniline has made the capping thick due to this particle size increased. Due to large particle size obtained for sample having 9 wt% polyaniline content the *quantum confinement effect* could not observed for this sample resulting in red-shift. The sizes of the particles calculated using the empirical formula [43] given by Equation (3) below:

$$2R = 0.1\ nm / (0.138 - 0.0002345\ \lambda_c) \qquad (3)$$

where 2R = particle's diameter, λ_c = absorption edge/absorption discontinuity. Calculated size of the particles is ~2 nm which was well agreement with XRD analysis.

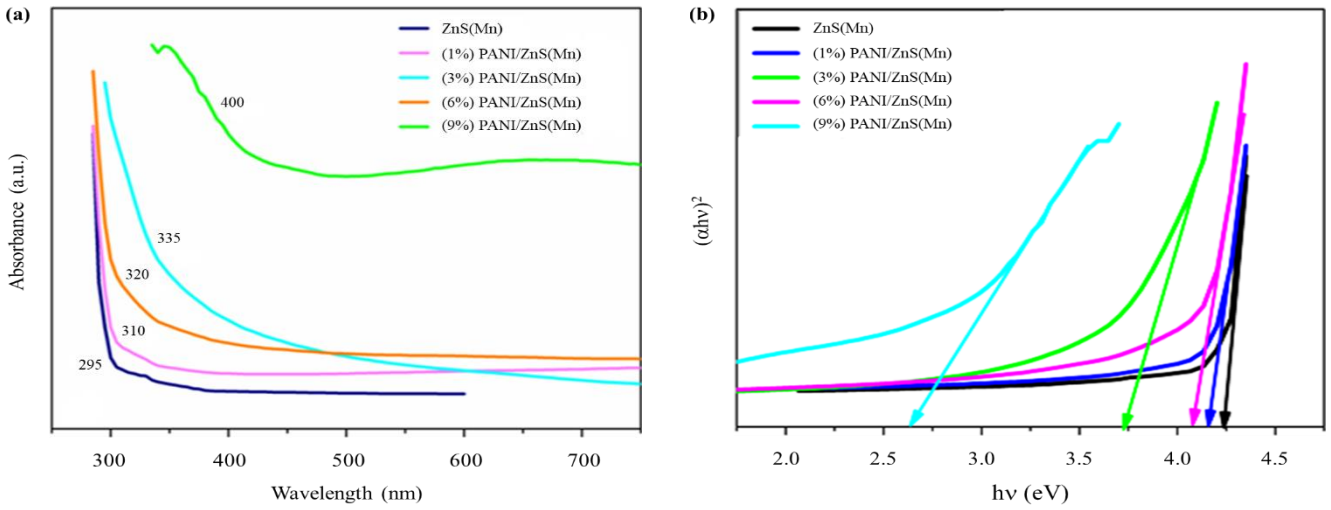

Figure 3. (a) Absorbance spectra (b) Tauc's plot of ZnS(Mn) and PANI capped ZnS(Mn) nanoparticles.

Table 1. Variation of optical direct bandgap energy and blue shift of ZnS(Mn), PANI capped ZnS(Mn) nanoaparticles, PANI capped ZnS(Mn) QDs.

Molar conc. of capping agent (PANI)	Direct bandgap energy (eV)	Blue shift (eV)
0%	4.2	0.54
1%	4.16	0.49
3%	3.73	0.06
6%	4.08	0.41
9%	2.6	------

3.4 Photoluminescence (PL) study

The PL spectra of uncapped ZnS(Mn) and PANI capped ZnS (Mn) nanoparticles has been shown in Figure 4. There are two sets of identifyable peaks observed at 308 nm and 607 nm which are associated with luminescence under ultraviolet band and orange band respectively. The orange emission around 607 nm can be originated from the $4T_1$–$6A_1$ transitions of Mn impurity ions [44]. The emission peak at 308 nm is accredited to the re-combination process of sulfur vacancies in the ZnS structure.

From both sets of PL peaks, it is observed that the height of peaks move towards red shift along with increasing PANI capping concentration (1%, 3%, 6%, 9%) when compare to uncapped ZnS(Mn) QDs. Thus, PL results show that the optical properties of zinc sulfide nanoparticles have remain present after polyaniline capping too.

3.5 HR-TEM analysis

HR-TEM analysis of uncapped ZnS(Mn) and PANI capped ZnS (Mn) QDs are shown in Figure 5. It is clearly observed from the HR-TEM micrograph particles of PANI capped ZnS(Mn) nanocomposite are not isolated but have agglomeration among them this may be due to the inter-particle interaction originating from the capped surface of PANI. For the long PANI chains, the dipole formations will not take place because during the growth of the PANI chains that the addition of monomer units neutralized the polarity on the attacking site of growing chain. But as the 1-dimensional growth of PANI chains is limited due to the entrapped ZnS(Mn) QDs, this brings re-distribution of surface charges on the polymer chains and ZnS(Mn) nanoparticles; the dipole formation on the ZnS(Mn) particles cause the interaction among capped particles leading to particles agglomeration. Figure 5(a) shows that the shape of ZnS(Mn) isolated particles are almost spherical and the size of ZnS(Mn) nanoparticles are analyzed by the use of Image J. The particle size distribution has been done by Gaussian curve which can be observed from Figure 5(c).

The estimated size of the particles from HR-TEM analysis is 2.5 nm, which is very close to exciton radius of Bohr's, which is well in agreement to size calculated with absorption spectra and XRD. Also TEM image in Figure 5(b), confirms that ZnS particles are well entrapped in the polyaniline matrix.

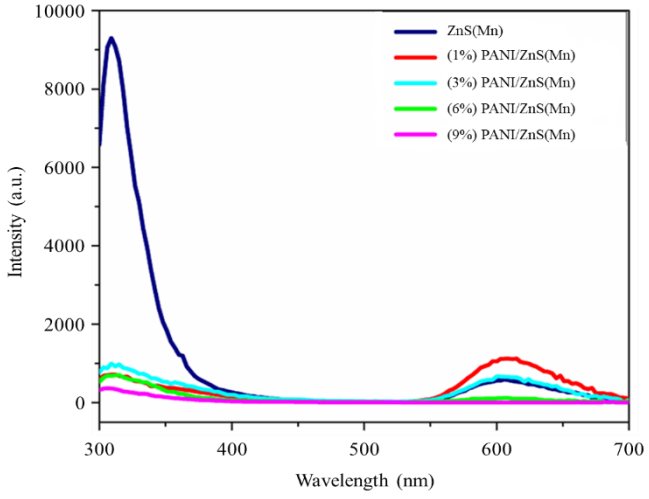

Figure 4. PL spectra of uncapped ZnS(Mn) and PANI capped ZnS(Mn) nanoparticles.

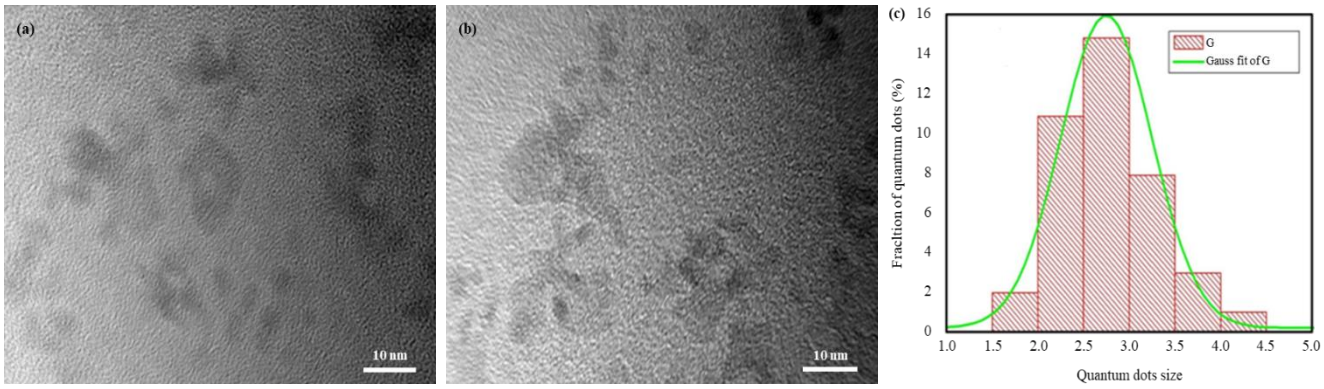

Figure 5. HR-TEM micrograph (a) Uncapped ZnS(Mn) (b)PANI capped ZnS(Mn) and(c) Particle size distribution.

3.6 Theoretical calculation

The electrostatic potential surface analysis of PANI and ZnS is performed using surface analysis by DFT (B3LYP) 6-31G in the department of Physics, MMEC, MMDU. Surface analysis of PANI shows that although the overall charge on the molecule is zero, the charge is not evenly distributed over the entire molecule. The N positions have electronegative sites while H_{13}, H_{25} and H_{37} are the most electropositive sites of the molecule as shown in the Figure 6(a). It is high possibility that electronegative sites are being attacked by the electronegative species. Further, a simultaneous electrostatic potential surface analysis of ZnS and polyaniline shows a strong electronic interaction through N and Zn, which results in the bond formation between the ZnS and PANI. The strong affinity of Zn towards N is due to the large negative Mullikan atomic charge which is –0.853338 e^- on the N. So, it is concluded that interaction between PANI chains and ZnS is strongly favorable for the formation of bond which gives better stability to the PANI. The larger bond length of 2.40 Å was calculated between Zn and S for ZnS molecule as compared to 2.0818 Å for PANI/ZnS(Mn) nanocomposite. The structural instability shown by the larger bond length and generates defective sites of ZnS, which results enhanced optical properties of ZnS. The interaction of ZnS with PANI results in a significant negative charge (0.467199 e^-) on the S, turning this end significantly electronegative as shown in Figure 6(c), this S site has a stronger potential for attracting the electropositive sites of near PANI chains to cover ZnS.

Further, the electronegative sites were calculated over the plane of each benzene ring as shown in Figure 6(b). *Dipole moment* calculated for PANI is 2.7389 Debye and for PANI/ZnS(Mn) nanocomposites is 13.3586 Debye. The PANI/ZnS(Mn) nanocomposites higher dipole moment shows greater its structural when compared to PANI, results in a higher surface charge on the nanocomposite material. A large *dipole moment* creates the strong interaction among particles of PANI/ZnS(Mn) nanocomposite which results in the agglomeration of particles; this fact was also confirmed from the TEM images.

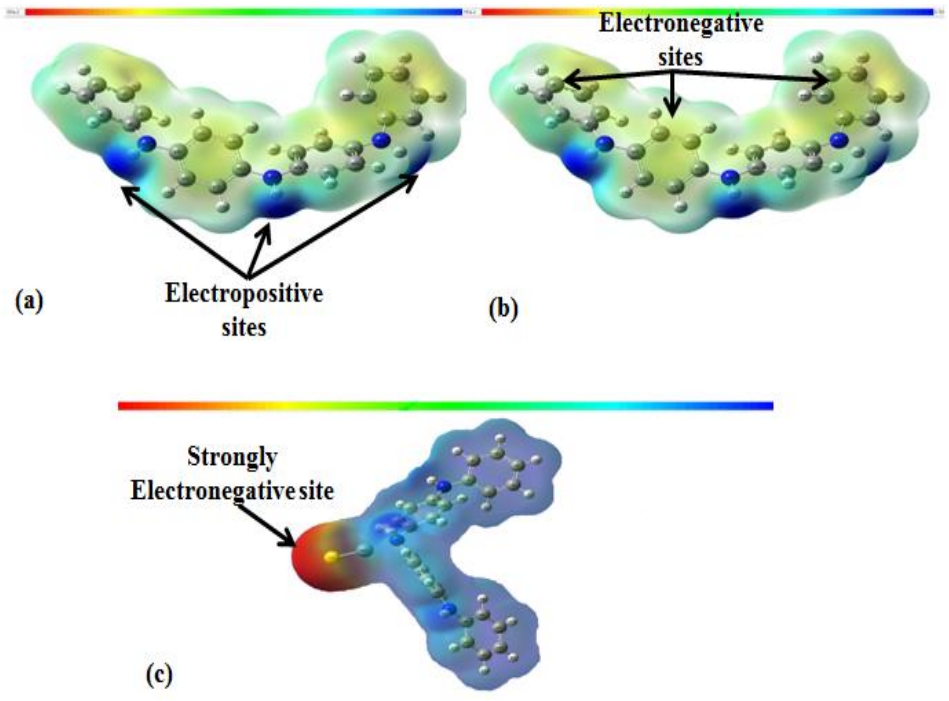

Figure 6. Optimized geometry of PANI **(**a) electro positive site, (b) electro negative site, and (c) ZnS attach with PANI.

4. Conclusion

ZnS(Mn) quantum dots are prepared using polyaniline as a capping agent by simple chemical method. From X-ray diffraction, the size of *quantum dots*, after PANI capping, is found to be very close to 2 nm which is nearly the same as bare ZnS(Mn) *quantum dots*. This reveals that no dilution of core particles occurs during the growth process of the PANI chains and the particle size is below exciton radius of Bohr. The particles size estimated from HR-TEM images using "image J" is found close to 2.5 nm for both the uncapped and capped samples. A slight agglomeration is observed under HR-TEM among the particles of PANI/ZnS(Mn) nanocomposite indicating that inter-particle interaction originates from polymer capping. The absorption spectra show the occurrence of the blue shift in wavelength peaks with enhanced bandgap of up to 6% of PANI in PANI/ZnS(Mn) nanocomposites that confirms the *quantum confinement effect*. Photoluminescence spectroscopy of the samples exhibit two sets of intensity peaks corresponds to 308 nm is due to sulfur vacancy and 607 nm corresponding to the $4T_1$-$6T_1$ transition of Mn. Strong dipole moment of 13.3586 Debye and larger bond length for Zn-S that creates asymmetry in the PANI/ZnS(Mn) nanocomposite. This asymmetry improves the PANI/ZnS(Mn) nanocomposite upto 6 wt% of PANI above these fraction optical properties diminished because of particle size increment. PANI capped ZnS(Mn) QDs show proper emission intensity in PL spectra and strong *quantum confinement* effect at the different concentrations of PANI in absorption spectra, this confirms that these nanoparticles can be used for diode laser applications [45] and foldable devices.

Acknowledgements

The author is thankful to Maharishi Markandeshwar University, Mullana,Ambala,Haryana and Indian institute of technology, Roorkee (Uttarakhand) for providing all research facilities.

References

[1] S. Singhal, J. Kaur, T. Namgyal, and R. Sharma, "Cu-doped ZnO nanoparticles: synthesis, structural and electrical properties," *Physica B: Condensed Matter*, vol. 407, no. 8, pp. 1223-1226, 2012.

[2] H. Bahramnia, H. M. Semnani, A. Habibolahzadeh, and H. Abdoos, "Epoxy/polyurethane hybrid nanocomposite coatings reinforced with MWCNTs and SiO_2 nanoparticles processing, mechanical properties and wear behavior," *Surface and Coatings Technology*, vol. 415, pp. 127121, 2021.

[3] A. Kumar, M. Kumar, V.Bhatt, D.Kim, S. Mukherjee, J. H. Yun, and R. K. Choubey, "ZnS microspheres-based photoconductor for UV light-sensing applications", *Chemical Physics Letters*, vol. 763, p. 138162, 2021.

[4] V. D. Mote, and B. N. Dole, "Structural, optical, and magnetic properties of Mn-doped ZnS nanoparticles," *Journal of Materials Science: Materials in Electronics*, vol. 32, no. 1, pp. 420-429, 2021.

[5] B. X. Dong, F. Qiu, Q. Li, S. L. Shu, H. Y. Yang, and Q. C. Jiang, "The synthesis, structure, morphology characterizations and evolution mechanisms of nanosized titanium carbides and their further applications," *Nanomaterials*, vol. 9, no. 8, p. 1152, 2019.

[6] S. Mallesh, and V. Srinivas, "Evolution of structure and magnetic properties in Mn Zn ferrite-silica nanocomposites fabricated by sol-gel method," *Journal of Materials Science: Materials in Electronics*, vol. 32, no. 4, pp. 4862-4871, 2021.

[7] A. Kumar, M. Kumar, V. Bhatt, S. Mukherjee, S. Kumar, H. Sharma, and R. K. Choubey, "Highly responsive and low-cost ultraviolet sensor based on ZnS/p-Si heterojunction grown by chemical bath deposition" *Sensors and Actuators A: Physical*, vol. 331, p.112988, 2021.

[8] J. Klanwan, N. Akrapattangkul, V. Pavarajarn, T. Seto, Y. Otani, and T. Charinpanitkul, "Single-step synthesis of MWCNT/ZnO nanocomposite using co-chemical vapor deposition method," *Materials Letters*, vol. 64, no. 1, pp. 80-82, 2010.

[9] N. Manivannan, S. K. CK, and R. Sathyamoorthy, "Effect of Gd doping on structural, surface and optical properties of ZnS prepared by chemical precipitation method," *Optik*, vol. 136, pp. 259-264, 2017.

[10] M. Hessien, E. Da'na, and A. Taha, "Phytoextract assisted hydrothermal synthesis of ZnO–NiO nanocomposites using neem leaves extract," *Ceramics International*, vol. 47, no. 1, pp. 811-816, 2021.

[11] M. R. Bodke, Y. Purushotham, and B. N. Dole, "Crystallographic and optical studies on Cr doped ZnS nanocrystals," *Cerâmica*, vol. 60, no. 355, pp.425-428, 2014.

[12] R. Kandulna, and R. B. Choudhary, "Robust electron transport properties of PANI/PPY/ZnO polymeric nanocomposites for OLED applications," *Optik*, vol. 144, pp. 40-48, 2017.

[13] K. R. Bindu, and E. I. Anila, "Optimized synthesis temperature and doping concentration of copper in zinc sulfide nanoparticles for green emission," *Materials Science in Semiconductor Processing*, vol. 121, p. 105317, 2021.

[14] A. Kumar, M. Kumar, V. Bhatt, D. Kim, S. Mukherjee, J. H. Yun, and R. K. Choubey, "ZnS microspheres-based photoconductor for UV light-sensing applications," *Chemical Physics Letters*, vol. 763, p. 138162, 2021.

[15] I. Hussain, D. Mohapatra, G. Dhakal, C. Lamiel, S. G. Mohamed, M. S. Sayed and J. J. Shim, "Different controlled nanostructures of Mn-doped ZnS for high-performance supercapacitor applications," *Journal of Energy Storage*, vol. 32, p. 101767, 2020.

[16] V. D. Mote, and B. N. Dole, "Structural, optical and magnetic properties of Mn-doped ZnS nanoparticles," *Journal of Materials Science: Materials in Electronics*, vol. 32, no. 1, pp. 1-10, 2020.

[17] A. Kumar, S. Mukherjee, S. Sahare, and R. K. Choubey, "Influence of deposition time on the properties of ZnS/p-Si heterostructures", *Materials Science in Semiconductor Processing*, vol. 122, p. 105471, 2021.

[18] A. Kaderavkova, L. Loghina, M. Chylii, S. Slang, P. Placek, B. Frumarova, and M. Vlcek, "N, N′, N′-trisubstituted thiourea as a novel sulfur source for the synthesis of Mn-doped ZnS QDs," *Journal of Alloys and Compounds*, vol. 831, p. 154814, 2020.

[19] K. P. Tiwary, F. Ali, S. K. Choubey, R. K. Mishra, and K. Sharma, "Doping effect of Ni^{2+} ion on structural, morphological

and optical properties of Zinc sulfide nanoparticles synthesized by a microwave-assisted method," *Optik,* vol. 227, p. 166045, 2021.

[20] A. Badawi, and M. G. Althobaiti, "Effect of Cu-doping on the structure, FT-IR and optical properties of Titania for environmental-friendly applications," *Ceramics International*, vol. 47, no. 8, pp. 11777-11785, 2021.

[21] M. Mostafa, J. El Nady, S. M. Ebrahim, and A. M. Elshaer, "Synthesis, structural, and optical properties of Mn^{2+} doped ZnS *quantum dots* for biosensor application," *Optical Materials,* vol. 112, p. 110732, 2021.

[22] B. Poornaprakash, U. Chalapathi, M. Kumar, S. P. Vattikuti, B. Rajitha, P. T. Poojitha, and S. H. Park, "Tailoring the optical and magnetic properties of ZnS nanoparticles via 3d and 4f elements co-doping," *Materials Science in Semiconductor Processing,* vol. 121, p. 105395, 2021.

[23] R. Sarkar, C. S. Tiwary, P. Kumbhakar, S, Basu, and A. K. Mitra, "Yellow-orange light emission from Mn^{2+}-doped ZnS nanoparticles," *Physica E: Low-dimensional Systems and Nanostructures,* vol. 40, no. 10, pp. 3115-3120, 2008.

[24] M. Nirmal, C. B. Murray, and M. G. Bawendi, "Fluorescence-line narrowing in CdSe quantum dots: Surface localization of the photogenerated exciton," *Physical Review B,* vol. 50, no. 4, p. 2293, 1994.

[25] M. Kuno, J. K.Lee, B. O. Dabbousi, F. V. Mikulec, and M. G. Bawendi, "The band edge luminescence of surface modified CdSe nanocrystallites: Probing the luminescing state," *The Journal of Chemical Physics,* vol. 106, no. 23, pp. 9869-9882, 1997.

[26] H. Shen, X. Bai, A. Wang, H. Wang, L. Qian, Y. Yang, and L. S. Li, "High-efficient deep-blue light-emitting diodes by using high quality ZnxCd1-xS/ZnS core/shell quantum dots," *Advanced Functional Materials*, vol. 24, no. 16, pp. 2367-2373, 2014.

[27] A. G. MacDiarmid, "Synthetic metal, a novel role for organic polymers (nobel lecture)," *Angewandte Chemie,* Int. Ed. vol. 40, pp. 2581-2590, 2001.

[28] R. Sehrawat, and A. Sil, "Effect of solvents on electrochemical performance of polypyrrole coated LiFePO 4/C cathode materials for Li-ion battery," *Journal of Materials Science: Materials in Electronics*, vol. 26, no. 7, pp. 5175-5185, 2015.

[29] Y. Li, S. Song, L. B. Zhang, X. X. Lian, L. X. Shan, and Q. J. Zhou, "Fabrication of hollow porous ZnO@ ZnS hetero-structures via the hydrothermal method and enhanced gas-sensing performance for ethanol," *Journal of Alloys and Compounds,* vol. 855, p. 157430, 2021.

[30] N. Arif, S. Gul, M. Sohail, S. Rizwan, and M. Iqbal, "Synthesis and characterization of layered Nb_2C MXene/ZnS nano-composites for highly selective electrochemical sensing of dopamine," *Ceramics International,* vol. 47, no. 2, pp. 2388-2396, 2021.

[31] H. Ali, "Ternary system from mesoporous CdS–ZnS modified with polyaniline for removal of cationic and anionic dyes," *Research on Chemical Intermediates,* vol. 46, no. 1, pp. 571-592, 2020.

[32] S. Saravanan, M. R. Anantharaman, S. Venkatachalam, and D. K. Avasthi, "Studies on the optical band gap and cluster size of the polyaniline thin films irradiated with swift heavy Si ions," *Vacuum,* vol. 82, no. 1, pp. 56-60, 2007.

[33] O. Bayram, "Conjugated polythiophene/Ni-doped ZnO hetero bilayer nanocomposite thin films: Its structural, optical and photoluminescence properties," *Ceramics International,* vol. 44, no. 17, pp. 20635-20640, 2018.

[34] S. Kumar, S. Taneja, S. Banyal, M. Singhal, V. Kumar, S. Sahare, and R. K. Choubey, "Bio-synthesised silver nano-particle-conjugated l-cysteine ceiled Mn: ZnS quantum dots for eco-friendly biosensor and antimicrobial applications", *Journal of Electronic Materials,* vol. 50, no. 7, pp. 3986-3995, 2021.

[35] M. L. Singla, R. Sehrawat, N. Rana, and K. Singh, "Dielectric behavior of emeraldine base polymer–ZnO nanocomposite film in the low to medium frequency," *Journal of Nanoparticle Research,* vol. 13, no. 5, pp. 2109-2116, 2011.

[36] M. Majhi, R. B. Choudhary, and P. Maji, "HCl protonated polymeric PANI-ZnS nanocomposites and measurement of their robust dielectric optical and thermal performance," *Optik,* vol. 136, pp. 181-191, 2017.

[37] S. Bousalem, F. Z. Zeggai, H. Baltach, and A. Benyoucef, "Physical and electrochemical investigations on hybrid materials synthesized by polyaniline with various amounts of ZnO nanoparticle," *Chemical Physics Letters,* vol. 741, p.137095, 2020.

[38] A. Bahrami, K. Behzad, N. Faraji, and A. Kharazmi," Electrical characteristics of PVA-PANI-ZnS nanocomposite film synthesized by gamma irradiation method," *Materials Science-Poland,* vol. 36, no. 1, pp.102-106, 2018.

[39] A. O. Ahmed, A. Alnehia, A. A. Qaid, H. T. Al-Ahsab, and A. Al-Sharabi, "Structural, morphological and optical properties of Cr doped ZnS nanoparticles prepared without any capping agent," *Optik*, vol. 214, pp.164831, 2020.

[40] H. R. Rajabi, and M. Farsi, "Study of capping agent effect on the structural, optical and photocatalytic properties of zinc sulfide quantum dots," *Materials Science in Semiconductor Processing*, vol. 48, pp. 14-22, 2016.

[41] S. Tomar, S. Gupta, S. Mukherjee, A. Singh, S. Kumar, and R. K. Choubey, "Manganese-doped ZnS QDs: An investigation into the optimal amount of doping", *Semiconductors,* vol. 54, no. 11, pp.1450-1458, 2020.

[42] S. Kumar, H. C. Jeon, T. W. Kang, R. Singh, J. K. Sharma, and R. K. Choubey, "Structural and optical properties of silica capped ZnS: Mn quantum dots", *Journal of Materials Science: Materials in Electronics,* vol. 26, no. 6, pp. 3939-3946, 2015.

[43] M. Rana, and P. Chowdhury, "L-glutathione capped CdSeS/ ZnS quantum dot sensor for the detection of environmentally hazardous metal ions," *Journal of Luminescence,* vol. 206, pp. 105-112, 2019.

[44] B. H. Zhang, F. Y. Wu, Y. M. Wu, and X. S. Zhan, "Fluorescent method for the determination of sulfide anion with ZnS: Mn quantum dots", *Journal of fluorescence,* vol. 20, no. 1, pp. 243-250, 2010.

[45] A. Y. Madkhli, and W. Shirbeeny, "The effect of cobalt ions doping on the optical properties of ZnS quantum dots according to photoluminescence intensity and crystalline structure," *Physica B: Condensed Matter,* vol. 597, p. 412414, 2020.